Comparison of Linear Primary Permanent Magnet Vernier Machine and Linear Vernier Hybrid Machine

Yi Du[1,2], Ming Cheng[2], K.T. Chau[3], Xianxing Liu[1], Feng Xiao[1], Wenxiang Zhao[1], Kai Shi[1], and Lihong Mo[1]

[1]School of Electrical and Information Engineering, Jiangsu University, Zhenjiang 212013, China
[2]School of Electrical Engineering, Southeast University, Nanjing 210096, China
[3]Department of Electrical and Electronic Engineering, University of Hong Kong, Hong Kong

This paper presents the comparison of linear primary permanent magnet vernier (LPPMV) machine and linear vernier hybrid (LVH) machine. The LPPMV machine and the LVH machine both operate based on the magnetic gear principle, hence possessing the advantages of low speed and high thrust force density. In addition, both machines employ similar configurations between which the key difference is that a one-piece primary iron core is employed in the LPPMV machine instead of the modular cores in the LVH machine. Using the finite element method (FEM), the characteristics and performances of two machines are analyzed and compared. The results show that the LPPMV machine exhibits higher thrust force and lower cogging force. Finally, the FEM results are validated by experiments based on a prototype of the LPPMV machine.

Index Terms— **Comparative study, high thrust force, linear machine, low speed, primary PM machine, vernier machine.**

I. Introduction

LINEAR permanent magnet (PM) machine with advantages of low speed and high thrust force are more and more attractive for direct-drive applications, such as ropeless elevator, railway traction, and wave energy conversion (WEC). Comparing with the conventional rotary-to-linearly drive system, the linear drive system possesses the merits of high efficiency and low initial and maintenance cost because of the absence of the linear-to-rotary device. However, the linear PM machine for direct-drive system usually suffers from a bulky size and a large number of poles because of the low-speed operation.

Recently, the concept of magnetic gears (MGs) based on the magnetic field modulation has been proposed in [1]. By adopting the coaxial topology, the MG offers some significant advantages, such as high transmission capability, physical isolation between input and output movers, minimum acoustic noise, improved reliability, maintenance-free operation, and inherent overload ability. Based on the MG or the MG principle, some special machines have been proposed to achieve the performances of low speed and high thrust force. In [2], a linear magnetic-geared PM machine is proposed for the direct-drive WEC by artfully integrating a linear MG with a linear PM brushless machine, which can achieve both low-speed motion and high-speed machine design simultaneously. However, it involves three airgaps, two moving parts, and an additional length that is caused by the series arrangement of the linear MG and the linear PM machine, thus suffering from the difficulty in manufacture. In [3], the PM vernier machine is developed, which employs the magnetic gearing effect, for the high torque density and low-speed application. The corresponding linear version is proposed for direct-drive WEC [4]. However, it suffers from the problems of mechanical integrity and thermal instability since the PMs are located on the translator.

Manuscript received March 4, 2014; revised April 9, 2014; accepted April 10, 2014. Date of current version November 18, 2014. Corresponding author: Y. Du (e-mail: duyie@ujs.edu.cn).

Color versions of one or more of the figures in this paper are available online at http://ieeexplore.ieee.org.

Digital Object Identifier 10.1109/TMAG.2014.2317805

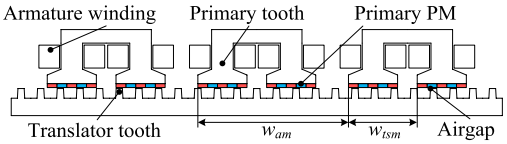

Fig. 1. Configuration of LVH machine.

To avoid the problems of mechanical integrity and thermal instability of the translator, the linear vernier hybrid (LVH) machine [5], [6] and the linear primary PM vernier (LPPMV) machine [7]–[9] have been proposed, in which the PMs are mounted on surface of the primary teeth. By employing the magnetic gearing effect, both of the LVH and LPPMV machines possess the merits of low speed and high thrust force and are suitable for the linear direct-drive system. However, a quantitative comparison between these two machines has not been reported.

The purpose of this paper is to compare the configurations, operation Principles, and performances of the LVH and LPPMV machines. In Section II, the configurations and the operation principles of the two machines will be described. In Section III, the characteristics of both machines will be analyzed and compared using the finite element method (FEM) with the same dimensions of PM block and the same slot current density. To verify the FEM results, a prototype of LPPMV machine is built and tested. Finally, conclusion will be drawn in Section IV.

II. Machine Configurations and Operation Principles

A. LVH Machine

Fig. 1 shows the configuration of the LVH machine in which the translator is designed as a simple iron core with salient teeth and the primary side is composed of modular U-shaped laminated iron cores with a coil wound on each primary tooth and PMs mounted on the teeth surface.

The width of single PM w_{PM} is equal to a half of the translator pitch τ_t, and the magnetization directions of the PMs on each single primary tooth are adjacent alternant.

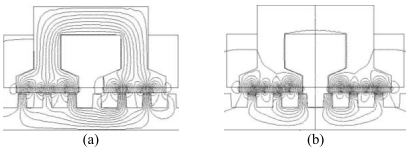

Fig. 2. No-load magnetic field distributions in LVH machine. (a) Position $A, \theta_e = 0°$. (b) Position $B, \theta_e = 90°$.

The relative displacement between the two primary teeth which belong to the same module is equal to 180° (electrical), as given by

$$w_{\text{tsm}} = m w_{\text{PM}} \tag{1}$$

where w_{tsm} is the mechanical distance between the two primary teeth which belong to the same module, m is an odd number when the magnetization directions of the PMs on these two teeth, respectively, are the same, and m is an even number when the magnetization directions of the PMs on these two teeth, respectively, are opposite.

Furthermore, to achieve a three-phase machine, the mechanical distance w_{am} between two U-shaped modules which belong to the adjacent phases can be expressed as

$$w_{\text{am}} = (n \pm 1/3)\tau_t \quad \text{or} \quad w_{\text{am}} = (n \pm 1/6)\tau_t \tag{2}$$

where n is a positive integer.

Actually, the operation principle of the LHV machine is very similar to that of the flux reversal PM machine. When the translator teeth are fully aligned with PMs, the flux linkage in the coil attains the maximum value, as shown in Fig. 2(a). As the translator moves, the flux linkage decays gradually until zero at the unaligned position, as shown in Fig. 2(b) and then reverses the polarity. Thus, a rapid change of the flux linkage polarity can be achieved over a short translator displacement, and the thrust force density can be improved consequently, which is so called the magnetic gearing effect.

B. LPPMV Machine

The configuration of LPPMV machine is very similar to that of LHV machine. As shown in Fig. 3, the key difference is that a one-piece laminated primary iron core is employed in the LPPMV machine instead of the modular cores in the LVH machine.

The LPPVM machine is operated based on the MG principle. The translator teeth function to modulate the magnetic field produced by the PMs on the primary teeth to get the effective magnetic field which links the winding effectively. In addition, the relationship among the pole pair of the PM magnetic field p_{PM}, the active number of the translator teeth n_t and the pole pair of the effective magnetic field p_{ef} can be expressed as

$$P_{\text{ef}} = \left| P_{\text{PM}} - n_t \right|. \tag{3}$$

Because the electrical speed of the translator is equal to the electrical speed of the effective flux, the mechanical speed of the effective flux can be obtained as

$$v_{\text{ef}} = \frac{n_t}{n_t - P_{\text{PM}}} v_t = G_r V_t. \tag{4}$$

In addition, the pitch of the effective flux can be written as

$$\tau_{\text{ef}} = \frac{1}{2} G_r \tau_t \tag{5}$$

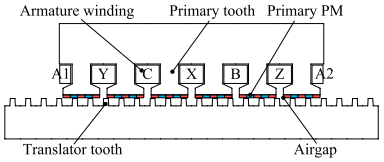

Fig. 3. Configuration of LPPMV machine.

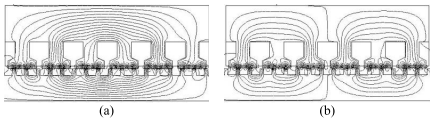

Fig. 4. No-load magnetic field distributions in LPPMV machine. (a) Position $A, \theta_e = 0°$. (b) Position $B, \theta_e = 90°$.

where v_{ef} and τ_{ef} are the mechanical speed and the pitch of the effective flux, v_t and τ_t are the mechanical speed and the tooth pitch of the translator, and G_r is the MG ratio.

The no-load magnetic field distributions at two typical translator positions are shown in Fig. 4. It can be found from (3) and Fig. 4 that the moving speed of the effective flux is increased to G_r times that of the translator due to the magnetic gearing effect, thus improving the thrust force.

In addition, it can be found from Fig. 4 and (5) that the design of the armature winding is just similar to the conventional PM synchronous machine with the pole-pair number of p_{ef}, which is another difference between the LPPMV and LVH machines.

III. Electromagnetic Performance Comparison

To quantitatively compare the electromagnetic performance, the LVH machine and the LPPMV machine are designed. The corresponding key parameters are listed in Table I. To enable a fair comparison between the two machines, the dimensions of the PM block, the slot current density and the slot height of the two machines are selected to be same.

Because the distributed winding is adopted in the LPPMV machine, the flux in the iron core is much larger than that in the LHV machine due to the field of the armature current, which results in thicker primary and translator yokes, and wider primary teeth in the LPPMV machine to avoid excessively high flux density. Therefore, a larger slot can be obtained in the LVH machine and more winding turns are allowed under the conditions of the same slot current density. It should be noticed that p_{ef} of the LPPMV machine is designed to be unity to achieve the thrust force as high as possible.

Using the FEM, the static characteristics of both machines are analyzed and compared. Fig. 5 compares the no-load flux linkage waveforms of the two machines. It can be seen that the peak-to-peak values of the LHV and LPPMV machines are equal to 0.28 and 0.4 Wb, respectively, in spite of more winding turns in the LVH machine.

The no-load electromotive force (EMF) waveforms can be obtained by differentiating the no-load flux linkage. As shown in Fig. 6, the peak value of the EMF of the LVH and LPPMV machines can achieve 40 and 60 V at the rated speed of 1 m/s. It can be found that the no-load EMF waveforms of the LPPMV machine are very sinusoidal of which the THD is about 2.5%. However, the THD of the LVH machine is more than 6.3%, which will result in large ripple of the thrust force.

TABLE I
QUANTITATIVE COMPARISON OF LVH AND LPPMV MACHINES

Parameters	LVH	LPPMV
Rated current, *RC* (A)	13	
Magnet remanence, B_r (T)	1.2	
PM number per primary tooth, N_{PMpt}	5	
Armature windings per phase, T_{pp} (Turn)	204	142
Thickness of primary yoke, h_{py} (mm)	14	55
Height of primary tooth, h_{pt} (mm)	27	
Height of primary pole shoe, h_{pps} (mm)	15	
Thickness of PMs, h_{PM} (mm)	4	
Height of secondary tooth, h_{st} (mm)	11	
Thickness of secondary yoke, h_{sy} (mm)	18	45
Width of primary tooth, w_{pt} (mm)	22	25
Width of primary slot, w_{ps} (mm)	24	17.5
Width of module, w_m(mm)	140	/
Gap between adjacent modules, g_{am} (mm)	20/3	/
Primary pitch, τ_p (mm)	70	60
Secondary pitch, τ_t (mm)	20	21.18
Airgap, *g* (mm)	1	
Magnetic gear ratio, G_r	/	17
Active length of motor, L_a (mm)	433.33	360
Thickness of motor, h_a (mm)	90	158
Volume, V_a (cm^3)	3900	5688
Shear stress, F_s (kN/m^2)	27.4	45
Thrust force density, F_v (kN/m^3)	305	285

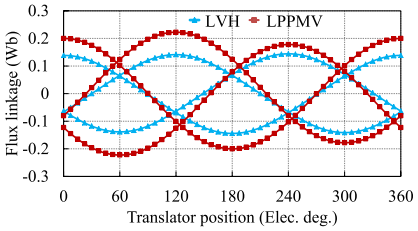

Fig. 5. Comparison of three-phase flux linkage waveforms.

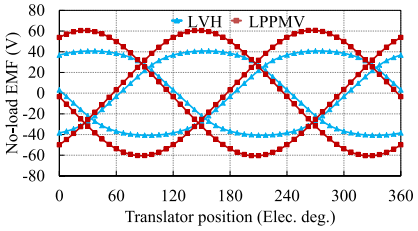

Fig. 6. Comparison of three-phase no-load EMF waveforms at 1 m/s.

When the $i_d = 0$ control method is adopted, the thrust force waveforms of both of the two machines can be obtained. As shown in Fig. 7, the average thrust forces of the LVH and LPPMV machines equal 1188 and 1621 N, respectively. It should be mentioned that the thrust force can be further improved because the iron core flux density is designed to be about 1.2 T to avoid excessively high iron loss during the overload situation.

Defining the shear stress F_s and thrust force density F_v as

$$F_s = \frac{F}{S_{\text{ag}}} \quad \text{and} \quad F_v = \frac{F}{V_{\text{a}}} \tag{6}$$

where F is the thrust force, S_{ag} is the active airgap area, and V_{a} is the active machine volume. The results obtained from (6) are listed in Table I. It confirms that the LPPMV machine can achieve higher shear stress which is 1.6 times that of the LVH machine. However, due to the thicker yoke of the iron core, the thrust force density of the LPPMV machine is slightly lower than that of the LVH machine. Moreover, the ripple of the LHV machine thrust force is obviously larger, of which the peak-to-peak value is about 76 N, and that of the LPPMV machine equals 49 N.

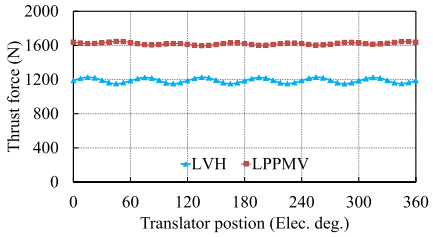

Fig. 7. Comparison of thrust force waveforms.

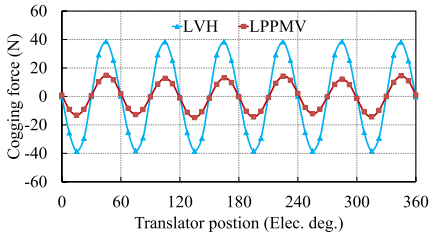

Fig. 8. Comparison of cogging force waveforms.

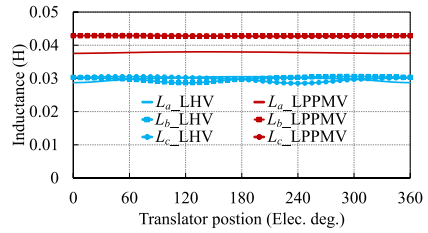

Fig. 9. Comparison of self-inductance waveforms.

Then, the corresponding cogging force waveforms of the two machines are shown in Fig. 8, which indicates that the peak-to-peak value of the cogging force of the LVM machine is 77 N, which is about 2.6 times that of the LPPMV machine.

The inductance of the PM vernier machine is usually large, so the power factor of this kind of machine is very low generally. The self-inductance waveforms of the two machines are compared in Fig. 9, and the mutual inductance of the LPPMV machine is shown in Fig. 10. It can be found that the inductance ripples with respect to the position of the translator is small enough to be ignored in both machines. In addition, the self-inductance of the LPPMV machine of phase A is smaller than that of phase B and phase C, and the absolute value of mutual inductances that are relative to phase A is smaller than the others because of the asymmetry of the armature winding and the end effect of the linear machine. However, due to the modular structure of the LVH machine, the three-phase self-inductance is almost the same and the mutual inductance almost equals zero.

To validate the FEM analysis, a prototype of the LPPMV machine is built, as shown in Fig. 11. The no-load EMF waveforms are measured by driving the primary at the rated speed of 1 m/s, as shown in Fig. 12. It can be seen that there is a good agreement with the FEM result. The difference between the experimental result and

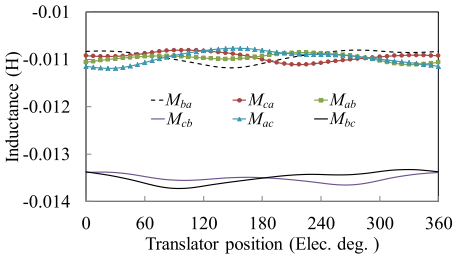

Fig. 10. Mutual inductance waveforms of LPPMV machine.

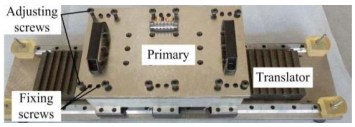

Fig. 11. Prototype of LPPMV machine.

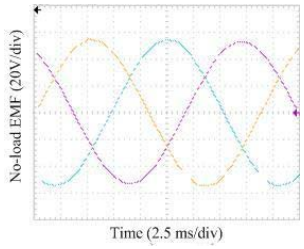

Fig. 12. Measured no-load EMF at 1 m/s of LPPMV machine.

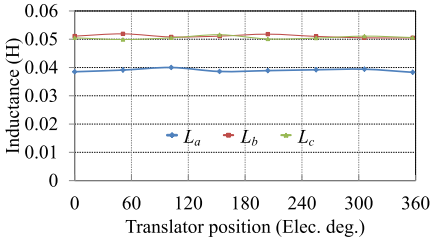

Fig. 13. Measured self-inductance waveforms of LPPMV machine.

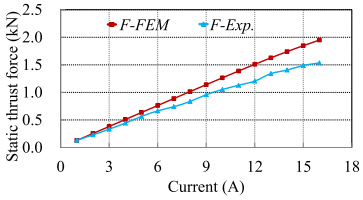

Fig. 14. Static thrust force versus armature current of LPPMV machine.

the FEM result is about 4 V, which is about 6.7% of the FEM results. It is mainly caused by the end effect, manufacturing imperfection and the measurement error. Fig. 13 shows the measured self-inductance waveforms of the LPPMV machine versus the translator position. It can be seen that the three-phase self-inductances are almost constants that are consistent with the FEM results. In addition, the measured inductance values are somewhat bigger than the FEM results because the 2-D FEM has not considered the end leakage.

The static thrust force is measured to estimate the force performance of the LPPMV machine when the armature current is in phase with the no-load EMF. Fig. 14 shows the measured static thrust force of the LPPMV machine versus the armature current. It can be seen that the trend of the thrust force is consistent with the result of FEM. However, the measured thrust force is slightly smaller than that of the FEM because the fixing position of the mover may be changed under the electromagnetic force due to the deformation of the connections, including the tension sensor. The thrust force can achieve 1390 N at the rated current, which is 86% of the value obtained from the FEM.

IV. Conclusion

In this paper, two new classes of linear PM vernier machines, namely the LVH and LPPMV machines, have been compared, including the machine configurations, operation principles, and electromagnetic performances. Using the FEM, the steady-state characteristics have been investigated. The analysis results confirm that the LPPMV machine can offer higher shear stress, lower thrust force ripple, and lower cogging force than the LVH machine. In addition, the LVH machine possesses the advantages of higher thrust force density and low inductance compared with the LPPMV machine. Therefore, the LPPMV machine is preferable for the low speed and high thrust force application in which the working area is limited. Finally, the prototype of the LPPMV machine is built and test. The experimental results have verified the analysis results using the FEM.

Acknowledgment

This work was supported in part by the National Natural Science Foundation of China under Project 51307072, Project 51277194, and Project 61174055, in part by the Academic Program Development of Jiangsu Higher Education Institution, and in part by Jiangsu University under Project 13JDG111 and Project 13JDG047.

References

[1] K. Atallah and D. Howe, "A novel high-performance magnetic gear," *IEEE Trans. Magn.*, vol. 37, no. 4, pp. 2844–2846, Jul. 2001.

[2] W. Li, K. T. Chau, and J. Z. Jiang, "Application of linear magnetic gears for pseudo-direct-drive oceanic wave energy harvesting," *IEEE Trans. Magn.*, vol. 47, no. 10, pp. 2624–2627, Oct. 2011.

[3] A. Toba and T. A. Lipo, "Novel dual-excitation permanent magnet Vernier machine," in *Proc. 34th IEEE IAS Annu. Meeting*, Oct. 1999, pp. 2539–2544.

[4] W. Li, K. T. Chau, and C. H. T. Lee, "Challenges and opportunities of electric machines for renewable energy," *Progr. Electromagn. Res.*, vol. 42, pp. 42–74, Sep. 2012.

[5] N. Iwabuchi, A. Kawahara, T. Kume, T. Kabashima, and N. Nagasaka, "A novel high-torque reluctance motor with rare-earth magnet," *IEEE Trans. Ind. Appl.*, vol. 30, no. 3, pp. 609–614, May/Jun. 1994.

[6] M. A. Mueller and N. J. Baker, "Modelling the performance of the Vernier hybrid machine," *Proc. IEE—Electr. Power Appl.*, vol. 150, no. 6, pp. 647–654, Nov. 2003.

[7] Y. Du *et al.*, "Design and analysis of linear stator permanent magnet Vernier machines," *IEEE Trans. Magn.*, vol. 47, no. 10, pp. 4219–4222, Oct. 2011.

[8] J. Ji, J. Zhao, W. Zhao, Z. Fang, G. Liu, and Y. Du, "New high force density tubular permanent-magnet motor," *IEEE Trans. Appl. Supercond.*, vol. 24, no. 3, pp. 5200705-1–5200705-5, Jun. 2014.

[9] Y. Du, K. T. Chau, M. Cheng, Y. Fan, W. Zhao, and F. Li, "A linear stator permanent magnet Vernier HTS machine for wave energy conversion," *IEEE Trans. Appl. Supercond.*, vol. 22, no. 3, pp. 5202505-1–5202505-5, Jun. 2012.